Cancer Cell, Volume *30*

Supplemental Information

Oncolytic Virus-Mediated Targeting of PGE_2 in the Tumor Alters the Immune Status and Sensitizes Established and Resistant Tumors to Immunotherapy

Weizhou Hou, Padma Sampath, Juan J. Rojas, and Steve H. Thorne

Supplemental Data

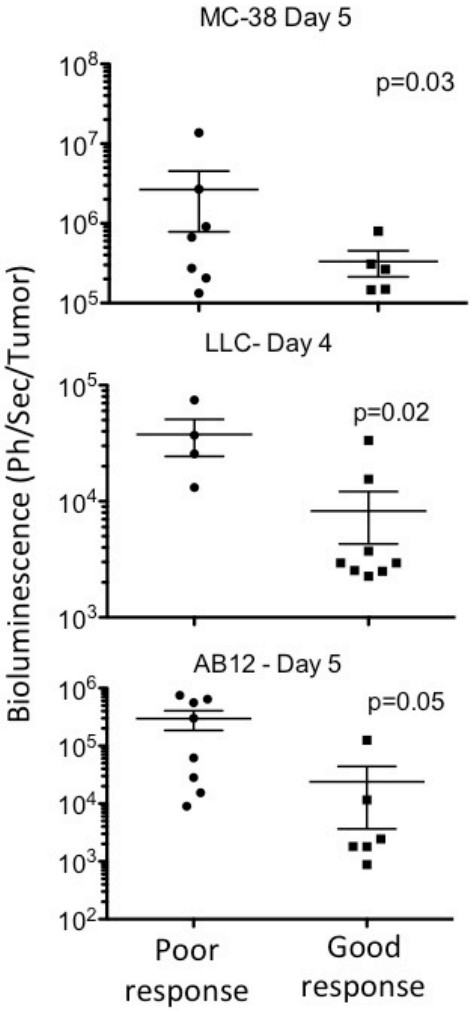

Figure S1, related to Figure 1. Tumor response corresponds to robust viral clearance at day 4/5 after treatment. Bioluminescence (viral luciferase gene expression) was detected on day 4 or 5 after treatment for several subcutaneous tumor–bearing immunocompetent mouse models (MC-38, LLC and AB-12) treated as described in Fig 1B. Within each model individual tumors are divided into good or poor responders and the viral gene expression from the tumor displayed for each group; Error bars ±SEM

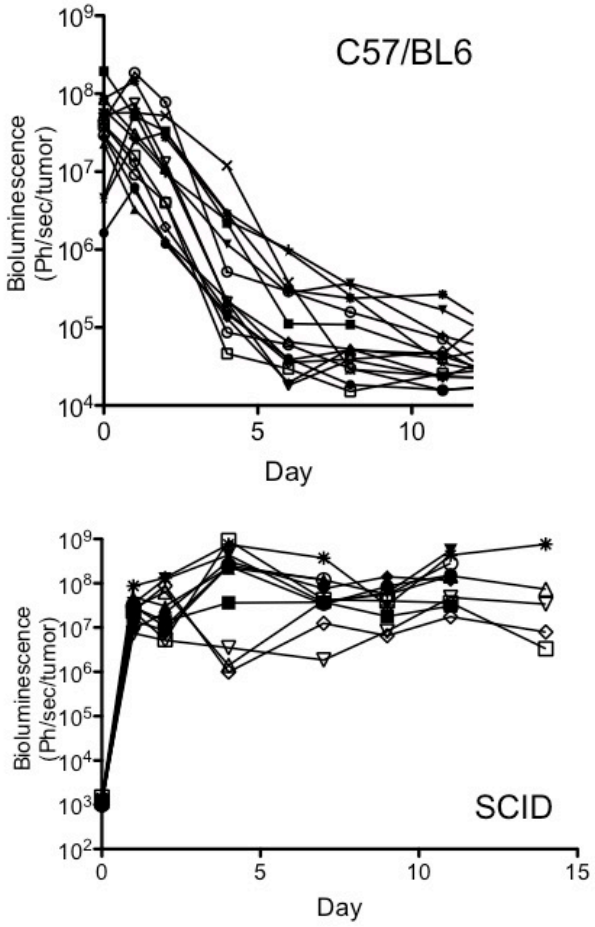

Figure S2, related to Figure 2. Enhanced viral clearance in immunocompetent mice**.** Viral gene expression (luciferase signal) from the tumor for individual mice bearing subcutaneous LLC tumors and treated with $1x10^7$ pfu WR.TK- IT. Immunocompetent (C57/BL6) and immunodeficient (SCID) mice are compared.

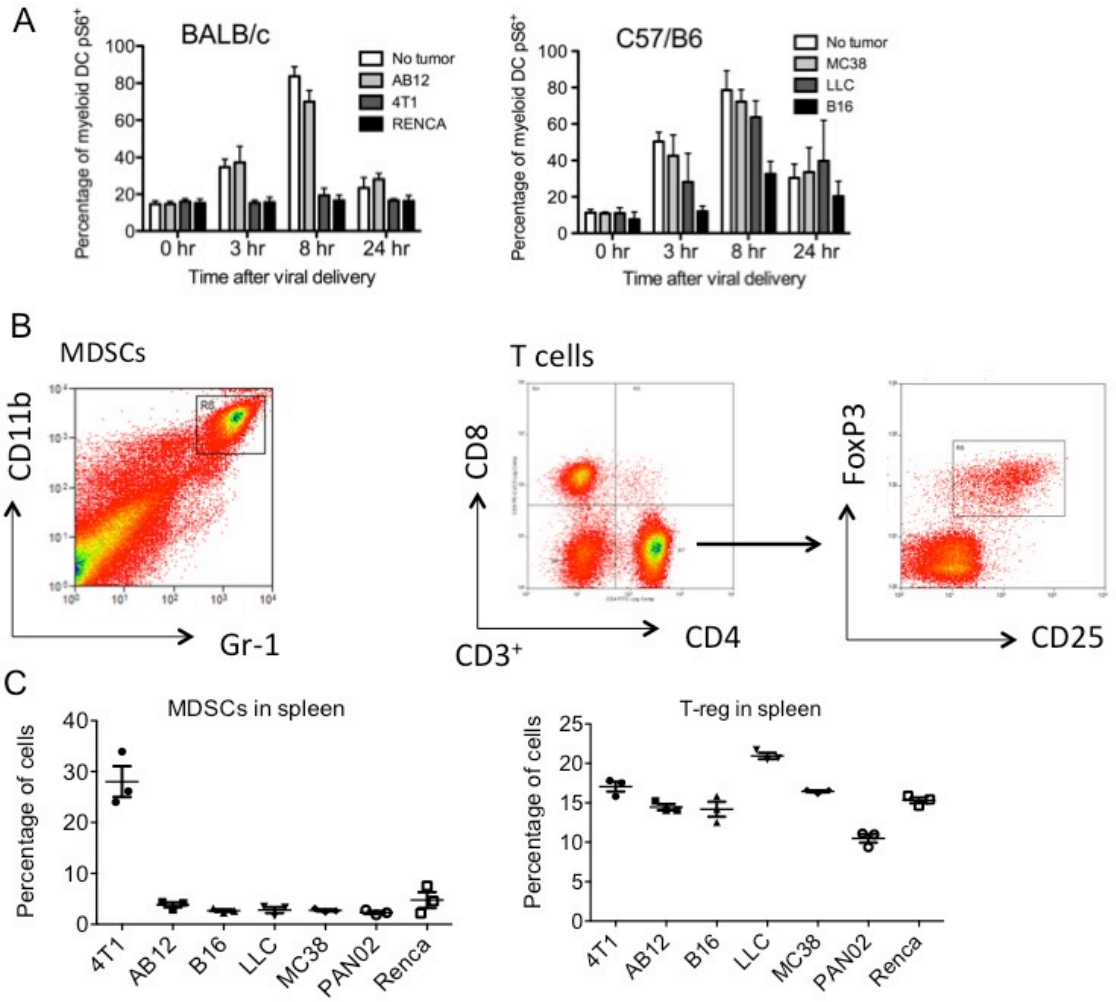

Figure S3, related to Figure 3. Analysis of levels and activation of immune cell subsets in the spleen. **(A)** Splenocytes were collected from mice with indicated tumors (or no tumor) at different times after intravenous (tail vein) injection of $1x10^8$ PFU of WR.TK- (n=3 per time point). Splenocytes were rapidly fixed and permeabilized and stained to examine pS6 levels in myeloid DCs ($CD11c^+CD11b^+B220^-CD8a^-$). 4T1, RENCA and B16 tumors displayed significant reduction ($p<0.05$) in pS6 levels at 3 hr and 8 hr post infection. **(B)** Gating strategies are shown for detection of MDSC (left) and T-cells and T-regs (right) for splenocytes or cells recovered from disaggregated tumors. **(C)** The levels of MDSC and T-reg in the spleen are shown for mice bearing different tumors. Error bars ±SEM

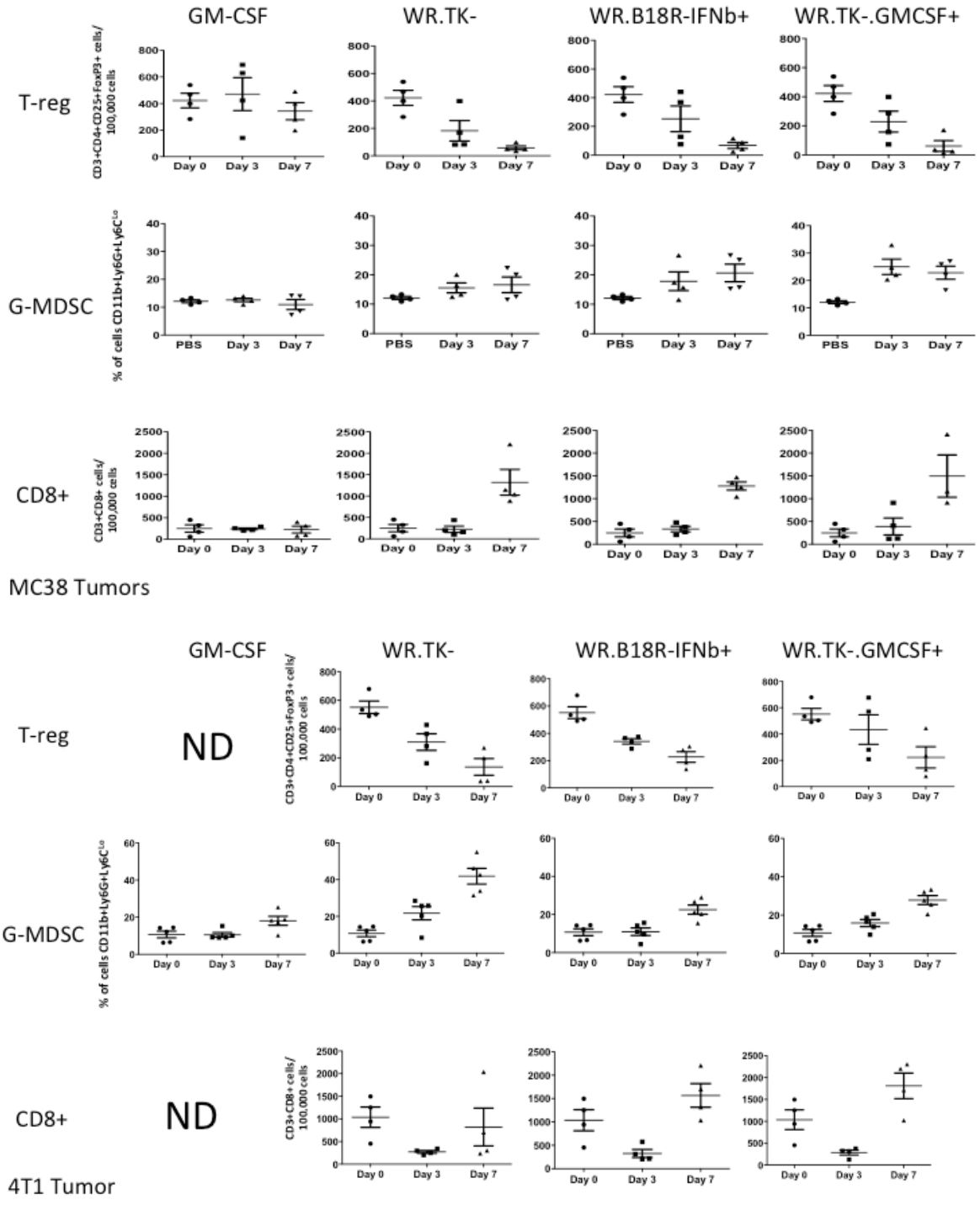

Figure S4, related to figure 3. Effect of different therapies on immune cell profiles in the tumor. Mice bearing MC38 (top) or 4T1 (bottom) tumors were treated and tumors recovered and analyzed as in Fig 2B. Only, in addition to WR.TK-, mice were also treated with recombinant mGM-CSF; WR.B18R-IFNb+; and WR.TK-GMCSF+. Error bars ±SEM

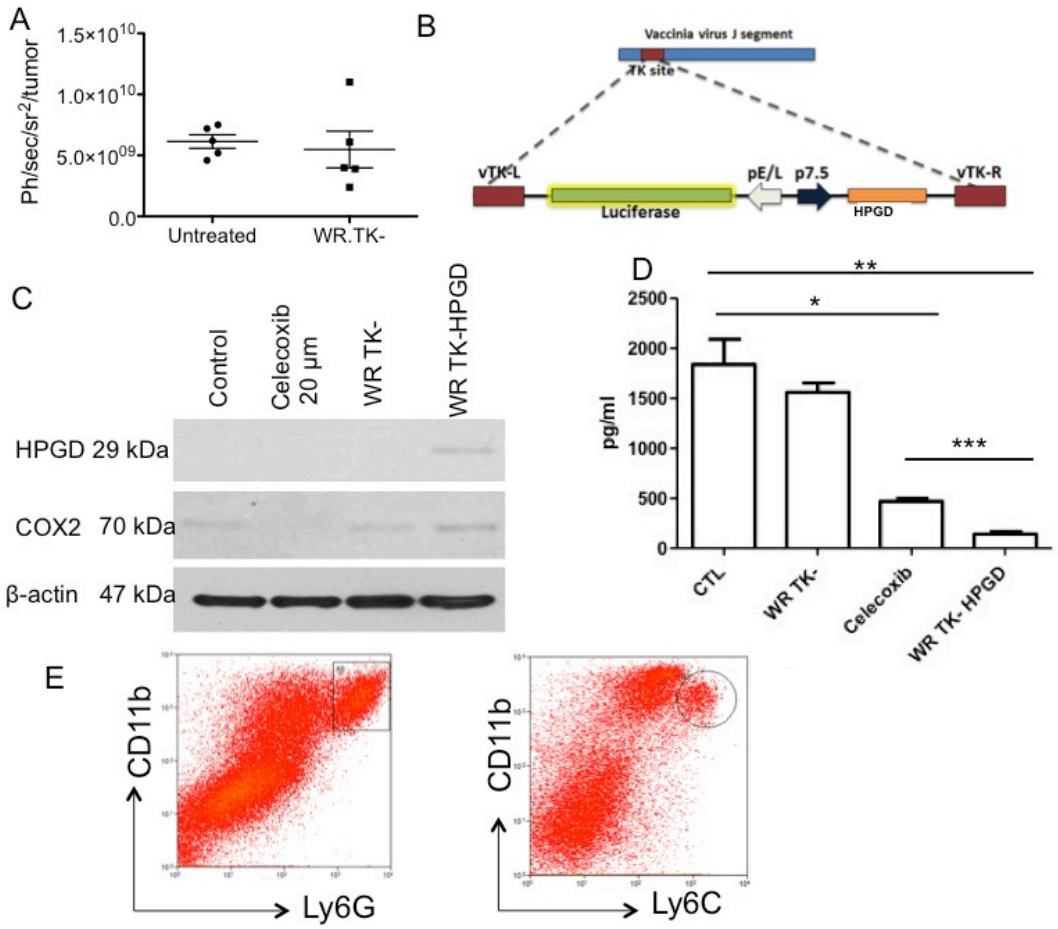

Figure S5, related to Figure 4. Targeting of COX2-PGE_2 pathway with an oncolytic virus to reduce MDSC in the tumor **(A)** Mice (nu-/nu-) bearing Renca tumors were treated with WR.TK- ($1x10^7$ PFU IT) or left untreated (n=5 per group) and COX2 expression was quantified in the tumors after addition of COX2 imaging reagent. Error bars ±SEM. **(B)** Diagram detailing the construction of WR.TK-HPGD+; **(C)** Mouse tumor (Renca) cells were collected 24 hr after infection with WR.TK-, WR.TK-HPGD+ or exposure to 20 µM celecoxib. Cells were treated with arachidonic acid for 4 hr before collection and lysis for Western blotting. Antibodies against HPGD (top), COX2 (middle) and beta-actin were used. **(D)** PGE_2 levels were also determined by ELISA in the media from Renca cells treated as before (* control (CTL) v celecoxib p=0.0017; ** CTL v WR.TK-HPGD+ p=0.0005; *** celecoxib v WR.TK-HPGD+ p=0.0002). Error bars ±SEM. **(E)** Representative plots to demonstrate gating strategy for defining granulocytic (top) and monocytic (bottom) MDSC in the tumor.

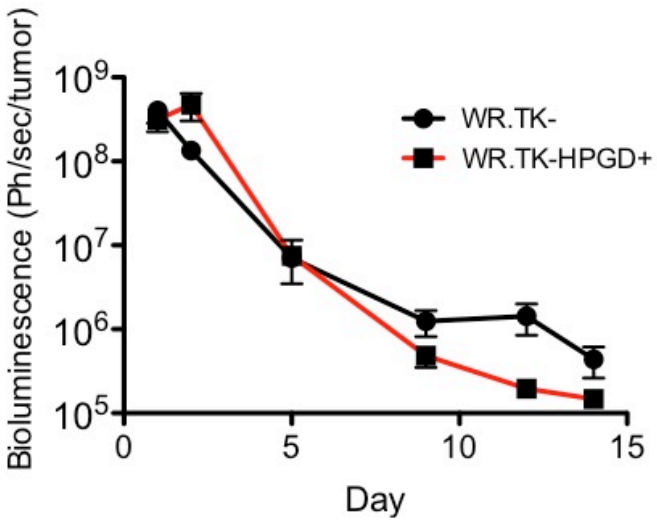

Figure S6, related to figure 5. Viral replication and persistence for vectors with and without HPGD transgene. Average bioluminescence signal from the tumors of mice (BALB/c bearing subcutaneous Renca tumors) after treatment ($1x10^7$ PFU IT) with WR.TK- or WR.TK-.HPGD+ (both expressing luciferase) (n=15 per group). Error bars ±SEM